Research Square

Preprints are preliminary reports that have not undergone peer review.
They should not be considered conclusive, used to inform clinical practice,
or referenced by the media as validated information.

Behavioral Clustering and Resting-State EEG Signatures of Transdiagnostic Neurodevelopmental Profiles

Emmanuelle Coutu-Nadeau

emmanuelle.coutu-nadeau@umontreal.ca

University of Montreal https://orcid.org/0009-0008-1628-7698

Vardan Arutiunian

University of Montreal

Charles-Olivier Martin

University of Montreal

Valérie K. Fontaine

University of Montreal

Anne-Marie Bélanger

University of Montreal

Khadije Jizi

https://orcid.org/0009-0005-2649-762X

Inga Sophia Knoth Knoth

Anthony Hosein

University of Montreal

Saeideh Davoudi

Laurent Caplette

University of Montreal

Hilda Bigdeli-Azari

University of Montreal

Marie-Laurence Brassard

University of Montreal

Julie Scorah

Carl Ernst

Montreal Neurological Institute https://orcid.org/0000-0002-2959-221X

Melissa Carter

Christine Lucas Tardif

Mélanie Couture

Pascale Abadie

Ridha Joober

Douglas Mental Health University Institute
Noémie Hébert-Lalonde
https://orcid.org/0000-0003-1552-3982
Guy Rouleau
McGill University, Montreal Neurological Institute-Hospital https://orcid.org/0000-0001-8403-1418
Mayada Elsabbagh
McGill University https://orcid.org/0000-0002-7311-9059
Baudouin Forgeot d'Arc
Sebastien Jacquemont
Université de Montréal https://orcid.org/0000-0001-6838-8767
Sarah Lippé
Department of Psychology University of Montreal, NED laboratory and Research Center UHC Sainte-Justine https://orcid.org/0000-0002-4430-1644

Article

Keywords:

Posted Date: August 26th, 2026

DOI: https://doi.org/10.21203/rs.3.rs-10692457/v1

License: This work is licensed under a Creative Commons Attribution 4.0 International License.
Read Full License

Additional Declarations: The authors have declared there is **NO** conflict of interest to disclose

Abstract

Autism spectrum disorder (ASD) and attention-deficit/hyperactivity disorder (ADHD) are highly heterogeneous neurodevelopmental disorders characterized by substantial phenotypic overlap and frequent co-occurrence. Traditional diagnostic categories may therefore fail to capture meaningful variation in symptom presentation. We investigated whether data-driven behavioral profiles derived independently of diagnosis correspond to distinct resting-state electroencephalography (EEG) signatures. A total of 237 children and adolescents (4.13–18.91 years) with ASD, ADHD, co-occurring ASD+ADHD, other neurodevelopmental conditions, or no diagnosis completed behavioral assessments and resting-state EEG recordings. Five behavioral measures reflecting social cognition, social communication, restrictive and repetitive behaviors, ADHD traits, and nonverbal IQ were entered into an unsupervised machine learning pipeline. Resting-state EEG spectral and nonlinear features were subsequently compared across clusters using linear models controlling for age and sex. A four-cluster solution was selected based on cluster stability and interpretability. The identified clusters were transdiagnostic, containing heterogeneous mixtures of diagnostic categories rather than diagnosis-specific groupings. The clusters differed in both symptom severity and behavioral profile. After false discovery rate correction, the most severe behavioral cluster exhibited significantly elevated periodic delta power, low- and high-gamma power, Hurst exponent, and Higuchi fractal dimension relative to the least severe cluster. No additional between-cluster EEG comparisons remained significant after correction. Our study suggests that neurodevelopmental heterogeneity may be better characterized by dimensional behavioral profiles than by diagnostic labels alone. Moreover, resting-state EEG features appear to track behavioral severity across neurodevelopmental conditions, supporting their potential utility as neurophysiological markers of transdiagnostic symptom severity.

INTRODUCTION

Neurodevelopmental disorders (NDDs) are a group of conditions characterized by early-arising disruptions in brain development leading to difficulties in personal, social, academic, or occupational functioning that persist throughout adulthood.[1] This broad category encompasses autism spectrum disorder (ASD), attention-deficit/hyperactivity disorder (ADHD), intellectual disability, communication, specific learning, motor disorders, etc.[1] Global epidemiological data indicate that ASD affects approximately 3% of the population[2–4] while ADHD affects between 5 to 7% of children worldwide.[5] Although the DSM-5 establishes discrete behavioral diagnostic criteria for these conditions, the clinical reality is one of high comorbidity across diagnoses and substantial heterogeneity within them.[6,7]

High rates of comorbidity between ASD and ADHD further blur the boundaries between diagnostic categories. Recent studies report that about 50 to 70% of children with ASD meet criteria for ADHD and about 10% of children with ADHD have a comorbid ASD diagnosis.[8–11] This high co-occurrence suggests that ASD and ADHD share underlying phenotypic dimensions rather than representing fully independent diagnostic entities. At the same time, phenotypic heterogeneity within each condition challenges the

assumption that a single diagnostic label captures a clinically uniform group. Within ASD alone, individuals vary substantially in language abilities, sensory profiles, or executive function.[12–14] Similar heterogeneity has been documented in ADHD, where symptom severity, cognitive profiles, and functional outcomes differ widely across individuals.[6,7,15] Together, these patterns indicate that categorical diagnostic labels alone are insufficient to capture the full phenotypic complexity of these NDDs. This has driven growing interest in identifying quantitative, neurophysiological biomarkers that can better characterize individual behavioral profiles.

Among candidate neurophysiological measures, electroencephalography (EEG) is a promising tool for developing those biomarkers as it provides a non-invasive, cost-effective measure of real-time neural activity from the scalp.[16–18] EEG signals can be characterized using both spectral measures, which quantify oscillatory activity across frequency bands[19–21] and nonlinear measures that capture complementary aspects of signal complexity and temporal dynamics.[22–24] The combined use of these two approaches provides a comprehensive characterization of brain function.[23,25] Resting-state EEG has already been widely used in the study of NDDs, revealing spectral alterations across ASD[18,26–28] and ADHD,[29–33].

In ASD, EEG studies have frequently described a U-shaped power profile characterized by increased power in low- and high-frequency bands alongside reduced power in intermediate frequencies.[6,18,27] Elevated gamma activity has also been linked to excitatory/inhibitory (E/I) imbalance, poorer language abilities in language-related tasks,[26,34,35] and specific behavioral traits in ASD.[17] Despite extensive efforts to identify an EEG signature of ASD, findings remain inconsistent and no clear consensus has emerged. This variability may reflect the substantial clinical heterogeneity of ASD, suggesting that multiple neurophysiological profiles may coexist within a single diagnostic category.[13,36]

In ADHD, resting-state EEG studies have often reported increased low-frequency activity, particularly in the theta band, alongside reduced alpha and beta activity. This pattern is often reflected in an elevated theta/beta ratio (TBR), which was long considered a potential biomarker of ADHD.[30] However, findings regarding the TBR have been inconsistent, and its validity as a diagnostic biomarker has been increasingly questioned.[37] More broadly, EEG findings in ADHD remain highly variable, and no single electrophysiological profile adequately characterizes all individuals with the disorder. This heterogeneity has led researchers to adopt transdiagnostic approaches that compare neurophysiological profiles across neurodevelopmental conditions rather than seeking biomarkers specific to a single diagnosis.[21,33,38,39]

Direct comparisons of resting-state EEG profiles between ASD and ADHD have begun to untangle both overlapping and disorder-specific patterns. Gamma-band oscillations have attracted increasing interest in neurodevelopmental research. Although evidence in ADHD remains limited and suggests reduced resting-state gamma activity,[37,40] studies in ASD more consistently report elevated gamma power and associations with greater behavioral symptom severity, lower cognitive functioning, and atypical sensory

processing.[26,35,41,42] Other frequency bands also show distinct or overlapping trends. Investigating power spectral density across children with ASD, ADHD, co-occurring ASD+ADHD, and typically developing (TD) controls, Shephard et al. (2018) demonstrated that spectral alterations in the comorbid group largely reflected a combination of characteristics observed in the single-diagnosis groups. Specifically, reduced theta (4–8 Hz) and alpha (8–12 Hz) power significantly characterized children with ASD, including those with comorbid ASD+ADHD. Conversely, reduced delta (0.5–3.5 Hz) power emerged as a shared marker of the ADHD, including the comorbid group. Most interestingly, they found some distinct variations in the comorbid ASD+ADHD group such as reduced theta relative to the ADHD-only group and reduced delta relative to TD.[39]

Beyond conventional spectral power, numerous studies have incorporated nonlinear measures of signal complexity and temporal dynamics, which may capture complementary aspects of atypical neurodevelopment.[25] In ASD, studies using entropy- and fractal-based approaches have identified differences in neural complexity relative to typically developing peers, although the direction of these effects has varied across metrics and developmental stages.[21,22,43,44] Similar alterations in EEG complexity have also been reported in ADHD, where greater fractal dimension and entropy have been interpreted as reflecting atypical neural dynamics and attentional regulation.[45] Together, these findings indicate that while ASD and ADHD each carry recognizable electrophysiological markers, their co-occurrence complicates the characterization. This pattern mirrors what has been found at the behavioral level: data-driven clustering of symptom profiles in mixed ASD and ADHD samples yields subgroups that have comparable proportions of children from both diagnostic categories.[6]

More recently, machine learning (ML) frameworks have been applied to behavioral data to discriminate between ASD and ADHD diagnoses with high accuracy.[46,47] In addition, ML has also been used in combination with EEG to help distinguish diagnostic categories from one another.[48–51] These studies have demonstrated that multivariate EEG features combined with data-driven classification methods can differentiate ASD from ADHD with greater accuracy than any single measure alone. However, a key limitation of these computational approaches is their persistent reliance on predefined diagnostic categories as the foundational ground truth. Whether behaviorally-derived profiles defined independently of diagnosis correspond to distinct EEG signatures across ASD, ADHD, and co-occurring presentations remains unexplored.

The current study addresses this gap by examining whether ML applied to behavioral data can uncover transdiagnostic profiles in children with NDDs, and whether these profiles are associated with distinct resting-state EEG signatures. Specifically, the study pursues two objectives: (1) to identify data-driven behavioral profiles across children with ASD, ADHD, and co-occurring ASD+ADHD diagnoses, regardless of their diagnostic label, and (2) to determine whether these profiles correspond to distinct electrophysiological features abstracted from the resting-state EEG.

METHODS

Participants

The final sample consisted of a total of 237 participants from Montreal Génétique des Familles and Quebec 1000 Families cohorts (age range 4.13–18.91 years, M = 11.02 +/- 3.38 years; 59.49% male, 73.42% White/European). Inclusion criteria for this study mandated that participants were under 19 years of age at enrollment and possessed a complete behavioral profile. Because participants were recruited at the family level, the sample includes sibling sets.

Diagnoses of participants were confirmed by their medical file upon recruitment. For all participants, the Autism Diagnostic Observation Schedule, Second Edition (ADOS-2)[52] was performed unless it had been done in the past. The assessment was conducted during the testing session to confirm ASD diagnoses. Given the presence of multiple and heterogeneous clinical labels in the dataset, diagnoses were parsed into broader categories reflecting the presence of ASD, ADHD, or both. Specifically, participants were classified into one of the following groups: *ASD* (n = 30, 12.66%), *ADHD* (n = 62, 26.16%), *ASD + ADHD* (n = 31, 13.08%), *ADHD + ASD-related behavioral traits* (n = 4, 1.69%), *Other neurodevelopmental conditions* (n = 17, 7.17%), or *No diagnosis* (n = 93, 39.24%).

All caregivers signed ethical consent forms and children and adolescents provided their assent. Ethics were approved by CHU Sainte-Justine.

Procedures

Testing sessions were conducted at either CHU Sainte-Justine or the Montreal Neurological Institute (MNI). Families were invited to come for a one-day testing session where each member would go through a series of questionnaires and EEG tasks.

Behavioral assessment

Nonverbal Intellectual Quotient (NVIQ). Non-verbal IQ was assessed for all participants. Different tests were used depending on the age and capacity of the participant. Adolescent participants (16+) were administered the Wechsler Adult Intelligence Scale, Fourth Edition (WAIS-IV).[53] Pediatric participants completed either the Wechsler Intelligence Scale for Children, Fifth Edition (WISC-V)[54] or the Wechsler Preschool and Primary Scale of Intelligence, Fourth Edition (WPPSI-IV)[55], depending on their age group. For participants requiring a completely non-verbal mode of assessment due to language deficits or specific developmental needs, the Leiter International Performance Scale, Third Edition (Leiter-3)[56] was utilized. All assessments were conducted during the laboratory visit. For the current analyses, only NVIQ scores were retained. NVIQ was derived from the Perceptual Reasoning Index (WAIS-IV), the Fluid Reasoning Index (WISC-V, WPPSI-IV), or the Leiter-3 Full Scale IQ, depending on the instrument used.

Social Responsiveness Scale (SRS). Social behavior was assessed using the SRS.[57] This scale consists of 65 items divided into 5 sections, each corresponding to one of the following subscales: Social Awareness, Social Cognition, Social Communication, Social Motivation, and Restrictive Interests and Repetitive Behavior (RRB). The total score ranges from 0 to 100 with a median of 50 and standard deviation of 10. The scale is designed for individuals aged 4 to 18. Each item describes a behavior (e.g. “Facial expressions don’t match speech”) and parents need to rate from 1 (False) to 4 (Always/almost always true) how much this behavior matches their child’s behavior in the past 6 months. For this study, only Social Cognition, Social Communication, and RRB categories (T-scores) were retained.

Achenbach System of Empirically Based Assessment (ASEBA). The Child Behavior Checklist (CBCL) versions of the ASEBA were completed by parents.[58] The CBCL consists of 99 items for children aged 1 to 5, and 112 items for children aged 6 to 18. Each item can be answered from 0 to 2 where 0 is “Not true”, 1 is “Sometimes true”, and 2 is “True or frequently true”. Multiple DSM-oriented scales are calculated based on the scores to the checklist items. In the current study, only the Attention Deficit/Hyperactivity T-score was retained for analysis.

EEG data acquisition and pre-processing

EEG signals were acquired using a 128-channel HydroCel Geodesic Sensory Net System with a 1000 Hz sampling rate. If necessary, younger children were invited to sit on their parent’s lap during the recording. In some cases, a research assistant was present in the recording room to ensure a proper unfolding. Resting-state was collected during a silent movie watching (3–5 minutes) for all participants.

Raw EEG files were exported from NetStation to MATLAB. Then, 20 electrodes corresponding to the outer edge of the cap were removed. The position of these electrodes makes them susceptible to artifacts from head movements, potentially resulting in a reduced signal-to-noise ratio. The Harvard Automated Preprocessing Pipeline for EEG (HAPPE Version3) was used to preprocess raw EEG signals from RS.[59] This pipeline is specifically optimized to address artifact contamination in pediatric datasets. First, a Notch filter was applied to remove line noise at 60 Hz.

Following initial noise suppression, the signal underwent bandpass filtering via a finite impulse response (FIR) filter with a passband of 1 to 80 Hz. Channels exhibiting poor signal quality due to elevated impedance, sensor displacement, or inconsistent scalp contact were detected through automated routines and excluded from the processing pipeline; these were subsequently interpolated in the final processing step. To further attenuate artifacts related to participants’ motion, electromyogenic activity, and ocular events (such as blinks or saccades), an optimized wavelet-enhanced independent component analysis (W-ICA) was applied, followed by an additional ICA step to remove any remaining muscle artifacts.

Since this study aimed to capture both spectral and non-linear complexity features, the cleaned data were segmented into 2-second and 5-second epochs to facilitate distinct feature extraction strategies.

Finally, segments with an amplitude exceeding +/- 150 μV were rejected.

Spectral features were extracted from non-overlapping 2-second segments. This epoch length was selected to ensure stationarity for Power Spectral Density (PSD) estimation while maximizing the number of available trials.[19] Spectral analysis was performed using custom Python scripts utilizing the MNE and FOOOF libraries. Features extracted included absolute PSDs – delta (1-3.99 Hz), theta (4-7.99 Hz), alpha (8-12.99 Hz), beta (13-29.9 Hz), and gamma (30–80 Hz) – and the Hurst exponent. Additionally, the fitting oscillations & one over f (FOOOF) parameterization algorithm was applied to obtain the periodic (oscillatory) and aperiodic components (exponent and offset) of the signal.[20]

To assess non-linear dynamics, nonlinear features were extracted from non-overlapping 5-second segments. This length was chosen to be long enough to capture meaningful physiological complexity patterns and stabilize entropy calculations.[60] Complexity features were extracted using the NeuroKit2 library and included the Higuchi fractal dimension and the Complexity Index (CI) derived from Multiscale Entropy (MSE) across both lowscale and highscale factors. This dual-segmentation approach allowed for a granular analysis of both the oscillatory and complexity profiles of the resting-state EEG. All extracted EEG features were averaged across channels to obtain a whole-head measure, yielding a single index for each spectral and non-linear metric.

Participants were excluded from the final analysis if they retained fewer than 30 artifact-free segments. This quality control procedure resulted in the exclusion of three participants (one due to insufficient 2-second segments, and two due to insufficient 5-second segments).

Clustering with Machine Learning

To identify data-driven behavioral groups within the sample, an unsupervised neural network approach using a Self-Organizing Map (SOM) was employed. All methods were implemented in Python (v3.13) using the *scikit-learn*, *numpy*, and *MiniSom* libraries. The feature space for clustering included five key behavioral dimensions: SRS Social Cognition, SRS Social Communication, SRS Restrictive and Repetitive Behavior, ASEBA ADHD T-scores, and NVIQ.

The SOM was implemented using the *MiniSom* library, with behavioral features transformed via a MinMaxScaler to a [0, 1] range. To ensure optimal model architecture, a targeted hyperparameter search evaluated combinations of learning rate (α = 0.3–0.5) and Gaussian neighborhood radius (σ = 0.5–1.5) that maximized silhouette score across potential cluster solutions (*k* = 2 to 8). A square grid of neurons was initialized based on the heuristic $5\sqrt{n}$ with random weight initialization and the network was trained over 2,000 iterations using the best-performing SOM configuration ($\sigma = 1.5,\ \alpha$ = 0.5) (Fig. 1).[61]

[FIGURE 1]

Model quality was further evaluated by calculating the Quantization Error (QE), which measures the average distance between each data point and its best-matching neuron, and Topographic Error (TE), which quantifies how well neighborhood relationships are preserved in the map. To derive discrete behavioral subtypes, *k*-means clustering was applied to the weights of the trained neurons. The final number of clusters was determined by evaluating the silhouette score and cluster stability. Stability was assessed by calculating the Adjusted Rand Index (ARI) across five independent *k*-means runs to assess consistency of participant assignment across clustering solutions. Additionally, soft-clustering membership probabilities were calculated for each participant based on the inverse Euclidean distance to the cluster centroids to account for clinical heterogeneity within the sample.

Statistical analysis

Normality of all behavioral measures was assessed using the Shapiro-Wilk test and an evaluation of skewness and excess kurtosis. Visual inspection of scatter plots confirmed the absence of significant univariate outliers. To investigate the neurophysiological differences between the identified clusters, we fitted a set of linear models with EEG features as dependent variables, cluster as a main effect, age and sex at birth were included in the models as covariates to control for developmental and sex-linked variance in brain activity. The structure of the model was as follows: *lm(EEG feature ~ Cluster + Age + Sex)*.

Cluster 4 was designated as the reference group for all models, as it represented the most clinically severe phenotype. A correction for multiple comparisons (false discovery rate, FDR) was applied to the analysis and significant *p*-values were corrected with the *p.adjust.method* in R. Finally, inter-feature relationships were explored using a Pearson correlation matrix.

Statistical analysis was performed in R (v4.5.1)[62] using *lm* for cluster-wise linear models. Additional summaries and diagnostics used packages including *dplyr*, *corrplot*, and *pheatmap* as implemented in the project scripts. Behavioral clustering and *k*-selection metrics were implemented in Python with *pandas*, *scikit-learn*, *MiniSom*, and *matplotlib* for diagnostic and selection plots. EEG features were derived from preprocessed data read with *MNE-Python* (including *EEGLAB-format epochs*). The complete preprocessing pipeline and integration scripts are hosted on GitHub at https://github.com/labo-NED/GENiAL/tree/genial-project-final.

RESULTS

Cluster Analysis

Identification of Behavioral Clusters

To determine the optimal clustering solution, model performance was evaluated across a range of cluster numbers (k = 2 to 8) and parameter configurations using silhouette scores and clustering stability (Adjusted Rand Index; ARI).[63] The final SOM achieved a Quantization Error (QE) of 0.1467 and a

Topographic Error (TE) of 0.0633, indicating a high level of representational accuracy and preservation of the data's topological structure.[64]

As *k* increased, silhouette scores gradually decreased, reflecting reduced separation between more fine-grained subgroups. While *k* = 2 provided the highest global silhouette score (0.41) and ARI (1.00), this solution primarily reflected a dichotomous split based on level of traits (i.e., high vs. low symptom load). To better capture the multi-dimensional heterogeneity of the sample and identify distinct behavioral profiles (e.g., social communication deficits without significant ADHD traits), higher order *k* values were evaluated (*k* > 2). While silhouette scores trended downward, clustering stability reached a local optimum at *k* = 4 (ARI = 0.98), representing an improvement over the *k* = 3 configuration (ARI = 0.96). Consequently, *k* = 4 was selected for the final analysis, as it maintained a meaningful silhouette score (0.30) while demonstrating near-perfect stability.

This value represented the highest level of granularity achievable before a significant decline in silhouette score and cluster stability was observed, allowing for a more detailed investigation into the relationship between behavioral subtypes and EEG features.

The demographic information for all four clusters can be seen in Table 1.

[TABLE 1]

Diagnostic Distribution Across Clusters

The distribution of clinical diagnoses within the whole sample and each group can be seen in Figs. 2a and 2b respectively.

Cluster 1 (N = 49) and Cluster 4 (N = 54) displayed the most heterogeneous diagnostic profile, with relatively balanced proportions across the diagnoses and no dominant diagnosis category. Cluster 2 (N = 85) was characterized by a strong dominance of the *No diagnosis* category. Cluster 3 (N = 49) showed a strong dominance for the *ADHD* diagnosis with almost half of the group falling in this category.

[FIGURE 2]

Between-cluster differences in behavioral measures

Mean behavioral scores across clusters are presented in Table 2.

[TABLE 2]

Clusters differed significantly across all behavioral measures, including SRS Restrictive and Repetitive Behaviors (RRB), SRS Social Communication, SRS Social Cognition, ADHD T-scores, and Nonverbal IQ (NVIQ). Figure 2c illustrates the distribution of behavioral scores across the behavioral clusters. Table 3 reports the result of the validation of the neural network-based stratifications.

In this study, we defined the most severe cluster as having the highest overall T-scores across RRB, SRS Social Communication, SRS Social Cognition, and ADHD traits, alongside the lowest NVIQ scores.

[TABLE 3]

EEG features

EEG analyses were conducted on a subset of participants with usable EEG data (N = 182 for 2s epochs and N = 165 for 5s epoch processing), resulting in reduced sample sizes compared to behavioral analyses. To investigate neurophysiological differences between subgroups, linear models were conducted with each EEG feature as dependent variables, cluster as the main effect (Cluster 4 as the reference) and age and sex as covariates. The reported *p*-values are FDR-corrected. The model outputs are shown in Table 4. Figure 2d illustrates the distribution of resting-state EEG features across the behavioral clusters.

The results showed that after correction for multiple comparisons, five EEG features retained their significance between clusters 2 and 4. Cluster 4, which represents the most severe behavioral phenotype, demonstrated significantly elevated Hurst exponent, Delta power, Low and High Gamma power, and Higuchi FD compared to Cluster 2, the least clinically severe group (Fig. 2d).

To further characterize the differences between clusters, post-hoc pairwise comparisons were performed across all EEG features. Results of this analysis were broadly consistent with the linear model findings, indicating that observed effects are primarily driven by differences involving Cluster 4 (most severe phenotype) and Cluster 2. No additional comparison remained significant after the FDR correction.

DISCUSSION

The present study aimed to investigate whether data-driven behavioral clustering could identify transdiagnostic profiles across children with neurodevelopmental disorders and whether these profiles are associated with distinct resting-state EEG signatures. Overall, we identified four stable behavioral clusters that captured meaningful heterogeneity across ASD, ADHD, and non-diagnosed children. Most importantly, the clusters created by the SOM algorithm were not driven by diagnostic categories, but rather by variations in levels of traits and behavioral profiles. Cluster 4 represented children with the lowest abilities in social cognition, social communication, NVIQ, and higher restrictive and repetitive behaviors and ADHD traits, and was further characterized by a distinct resting-state EEG profile. Together, these findings suggest that data-driven clustering can identify behaviorally and neurophysiologically meaningful subgroups that extend beyond traditional diagnostic boundaries.

Although some diagnostic categories were overrepresented in specific clusters, all groups included a mixture of ASD, ADHD, comorbid presentations, and non-diagnosed participants. This finding suggests that behavioral heterogeneity in neurodevelopmental conditions extends beyond traditional diagnostic

boundaries and may be better understood dimensionally rather than categorically, which aligns with an expanding body of recent findings.[6,7,13] The clinical reality of this diagnostic blending is supported by evidence of shared genetic predisposition between ASD and ADHD, which frequently manifest as overlapping neurocognitive characteristics and shared heritable traits.[11,65,66]

Furthermore, the presence of non-diagnosed participants across all clusters suggests that meaningful variation along these behavioral dimensions extends beyond individuals who meet formal DSM-5 diagnostic criteria. Some children who do not qualify for a categorical diagnosis may nevertheless exhibit elevated levels of social, attentional, or cognitive difficulties that place them closer to clinically diagnosed groups on specific behavioral dimensions. This observation highlights the potential value of considering symptom profiles beyond diagnostic status alone.[7,67]

To evaluate whether our data-driven behavioral cohorts correspond to distinct neural profiles, we examined resting-state EEG spectral and non-linear complexity metrics across the identified clusters. Our results showed that five neurophysiological features differentiated the two clinical extremes of the sample: Cluster 4, representing the most globally severe behavioral phenotype, and Cluster 2, representing the lowest-severity group.

Specifically, Cluster 4 demonstrated significantly elevated periodic delta power, low- and high-gamma power, Hurst exponent, and Higuchi FD relative to Cluster 2. Interestingly, despite the significant differences in behavioral characteristics across the four groups, only the two groups with severity extremes were significant in their EEG signatures. One possible explanation is that resting-state EEG metrics may be more sensitive to broad differences in overall trait severity than to finer-grained variations in behavioral presentation.[17,25,39]

Delta-band neural oscillations (1-3.99 Hz) have often been interpreted as a marker of atypical neurodevelopment, reflecting altered cortical maturation and cognitive dysfunction.[38,68] Consistent with those studies, we showed that the group characterized by the lowest social and cognitive abilities exhibited significantly elevated periodic delta power compared with the group with higher abilities. The selective elevation of delta power in Cluster 4 suggests that this feature may be more closely associated with overall levels of clinical traits than with any specific diagnostic category. Notably, although Clusters 1 and 4 displayed similarly heterogeneous diagnostic compositions, delta power did not significantly differentiate these groups. Together, these findings suggest that resting-state delta activity may be more closely related to the level of behavioral difficulties than to diagnostic status itself. *Gamma-band neural oscillations* (30–80Hz) are generally associated with attentional processes, perceptual binding, and top-down cognitive control in task-based protocols.[69,70] However, several resting-state EEG studies have reported elevated gamma power in autistic individuals compared with neurotypical controls, suggesting altered cortical network functioning and atypical neural synchronization.[18,71] One of the proposed mechanisms underlying atypical gamma activity is an imbalance between excitatory (glutamatergic) and inhibitory (GABAergic) neural signaling.[72,73] Such disruptions in excitatory/inhibitory (E/I) balance have

been widely implicated in the study of ASD and other neurodevelopmental conditions.[73–75] The elevated low- and high-gamma power observed in Cluster 4 may reflect altered cortical network regulation associated with lower behavioral abilities. The present findings are consistent with evidence linking atypical gamma activity to more significant neurodevelopmental difficulties including co-occurring conditions, such as language and cognitive impairments.[38,76]

The *Hurst exponent* is a non-linear measure that quantifies the fractal-like properties and self-similarity in the EEG signal, indicating the level of roughness in the time-series. Hurst exponent was estimated using rescaled range analysis (*R/S analysis*).[77] In EEG data, Hurst values greater than 0.5 indicate persistent dynamics, meaning that neural activity patterns tend to maintain similar trajectories over time rather than fluctuating randomly. Conversely, lower Hurst values reflect greater volatility and reduced predictability of the signal.[78] Our findings identified that Cluster 4 exhibited significantly elevated Hurst exponent values relative to Cluster 2. This suggests that neural activity in the group with the most clinical traits was characterized by greater temporal persistence and predictability. Previous work has proposed that elevated Hurst values may indicate stronger long-range temporal dependencies in neural activity, reflecting reduced dynamical flexibility, whereby neural systems become more constrained to particular activity states over time.[79] Within neurodevelopmental conditions, such alterations in long-range temporal structure have been associated with atypical information processing and network organization.[60] In line with this literature, the elevated Hurst exponent observed in Cluster 4 may indicate less flexible neural activity patterns associated with greater neurodevelopmental impairment.

Higuchi FD (HFD) is another non-linear measure that quantifies the complexity and irregularity of a time-series signal in the time domain. A higher HFD value indicates that the EEG signal is highly complex, less regular, and characterized by greater variability.[24,80] In the present study, Cluster 4 exhibited significantly elevated HFD values relative to Cluster 2, suggesting that the group with the most significant clinical traits displayed more variable neural dynamics.

While elevated HFD and Hurst exponent values may initially appear counterintuitive, these measures quantify different properties of neural dynamics. In theory, fractal dimension and the Hurst exponent are often expected to show an inverse relationship, such that greater temporal persistence is associated with lower signal irregularity. The inverse relation applies mainly to ideal self-affine/monofractal signals, not to EEG in general.[81] However, EEG signals are complex, non-stationary, and influenced by multiple frequency-specific and nonlinear properties, meaning that this theoretical relationship may not apply directly across all empirical contexts.[81] Consistent with this possibility, HFD and Hurst exponent were positively correlated in the present sample ($r = .557$, $p < .001$), suggesting that these features captured related but non-identical aspects of neural organization. HFD reflects the local complexity and irregularity of the signal, whereas the Hurst exponent captures its long-range temporal dependence.[23] Consequently, elevated values of both metrics are not necessarily mutually exclusive and may instead reflect alterations in multiple dimensions of neural organization.[82,83] The co-occurrence of elevated HFD, Hurst exponent, and gamma power in Cluster 4 may therefore indicate a distinct pattern of neural

dynamics involving both increased signal complexity and altered temporal structure. Rather than representing conflicting findings, this pattern suggests that the most behaviorally severe cluster is associated with a neurophysiological profile that cannot be captured by a single EEG metric alone.

Several limitations should be considered when interpreting the present findings. First, the clusters identified in this study were based solely on behavioral measures and should therefore be interpreted as behavioral phenotypes rather than biologically distinct subgroups. As a result, the present findings do not provide evidence regarding the underlying mechanisms of neurodevelopmental conditions and should not be interpreted as informing pharmacological or medical treatment decisions. Second, the inclusion of siblings within the sample may have influenced the observed clustering patterns, as related participants are more likely to share genetic and environmental characteristics than unrelated individuals. Consequently, some degree of non-independence between observations cannot be ruled out. Future studies should examine whether similar cluster structures emerge in fully independent samples.

Beyond advancing our understanding of neurodevelopmental heterogeneity, these findings may have important clinical implications. The present results suggest that children may be more meaningfully characterized by their behavioral profile and trait dimensions than by diagnostic labels alone. Although diagnostic categories remain essential for medical decision-making and access to services, data-driven approaches may ultimately contribute to more individualized assessment and intervention strategies by identifying clinically meaningful subgroups that cut across traditional diagnostic boundaries. Future research should examine the stability of these profiles over time, investigate whether interventions influence cluster membership, and explore the development of predictive models capable of identifying behavioral profiles at the individual level.

Declarations

FUNDING

The data and/or materials and/or registry resources used for this research were made available by the Quebec 1000 families (Q1K) project and through funds from the Fondation Marcelle et Jean Coutu and the Fonds de Recherche du Québec – secteur santé. The authors also wish to thank all families who contributed to the Q1K project.

This work was also supported by the Centre UNIQUE (Union Neurosciences & Artificial Intelligence – Québec), and the Canada Research Chair in Pediatric Neurodiversity (CRC-2024-00030).

DATA AVAILABILITY

The data that support the findings of this study are not currently publicly available due to participant privacy and ethical restrictions. The dataset is currently being prepared for controlled-access sharing through the Canadian Brain Imaging Data Governance and Sharing Platform (C-BIG). Until this process is complete, requests for access to the data should be directed to the corresponding author.

CODE AVAILABILITY

Analysis scripts are available at https://github.com/labo-NED/GENiAL/tree/genial-project-final.

COMPETING INTERESTS / CONFLICT OF INTERESTS

The authors declare no competing interests.

AUTHOR CONTRIBUTIONS

E.C.-N. conceptualized the study, curated the dataset, conducted the statistical analyses, interpreted the results, created the figures, and wrote the original manuscript draft.

V.A. contributed to the statistical analyses, interpretation of results, and manuscript preparation and revision.

C.-O.M., V.F., A.-M.B., K.J., and I.S.K. contributed to participant recruitment, data collection, and data management.

A.H. contributed to database development, maintenance, and data organization.

S.D. contributed to EEG preprocessing and feature extraction, assisted with data analysis, and contributed to manuscript revision.

J.S., N.H.-L., G.R., M.E., B.F.D., S.J., and S.L. contributed to study design, project supervision, funding acquisition, and manuscript revision.

S.L. supervised the project and provided overall scientific guidance throughout all stages of the study.

All authors reviewed, revised, and approved the final manuscript.

References

1. American Psychiatric Association. *Diagnostic and statistical manual of mental disorders*. American Psychiatric Association Publishing, 2022.
2. Lord C, Brugha TS, Charman T, Cusack J, Dumas G, Frazier T *et al.* Autism spectrum disorder. *Nat Rev Dis Primer* 2020; 6: 5.
3. Shaw KA. Prevalence and early identification of autism spectrum disorder among children aged 4 and 8 years—Autism and Developmental Disabilities Monitoring Network, 16 Sites, United States, 2022. *MMWR Surveill Summ* 2025; 74.
4. Zeidan J, Fombonne E, Scorah J, Ibrahim A, Durkin MS, Saxena S *et al.* Global prevalence of autism: A systematic review update. *Autism Res* 2022; 15: 778–790.
5. Cabral MDI, Liu S, Soares N. Attention-deficit/hyperactivity disorder: diagnostic criteria, epidemiology, risk factors and evaluation in youth. *Transl Pediatr* 2020; 9: S104-s113.

6. Deserno MK, Bathelt J, Groenman AP, Geurts HM. Probing the overarching continuum theory: data-driven phenotypic clustering of children with ASD or ADHD. *Eur Child Adolesc Psychiatry* 2023; 32: 1909–1923.
7. Thapar A, Cooper M, Rutter M. Neurodevelopmental disorders. *Lancet Psychiatry* 2017; 4: 339–346.
8. Canals J, Morales-Hidalgo P, Voltas N, Hernández-Martínez C. Prevalence of comorbidity of autism and ADHD and associated characteristics in school population: EPINED study. *Autism Res* 2024; 17: 1276–1286.
9. Leyfer OT, Folstein SE, Bacalman S, Davis NO, Dinh E, Morgan J *et al.* Comorbid psychiatric disorders in children with autism: Interview development and rates of disorders. *J Autism Dev Disord* 2006; 36: 849–861.
10. Simonoff E, Pickles A, Charman T, Chandler S, Loucas T, Baird G. Psychiatric disorders in children with autism spectrum disorders: prevalence, comorbidity, and associated factors in a population-derived sample. *J Am Acad Child Adolesc Psychiatry* 2008; 47: 921–929.
11. Hours C, Recasens C, Baleyte JM. ASD and ADHD Comorbidity: What Are We Talking About? *Front Psychiatry* 2022; 13: 837424.
12. Demetriou EA, Lampit A, Quintana DS, Naismith SL, Song YJC, Pye JE *et al.* Autism spectrum disorders: a meta-analysis of executive function. *Mol Psychiatry* 2018; 23: 1198–1204.
13. Lombardo MV, Lai M-C, Baron-Cohen S. Big data approaches to decomposing heterogeneity across the autism spectrum. *Mol Psychiatry* 2019; 24: 1435–1450.
14. Tillmann J, Uljarevic M, Crawley D, Dumas G, Loth E, Murphy D *et al.* Dissecting the phenotypic heterogeneity in sensory features in autism spectrum disorder: a factor mixture modelling approach. *Mol Autism* 2020; 11: 67.
15. Al-Saoud S, Nichols ES, Brossard-Racine M, Wild CJ, Norton L, Duerden EG. A transdiagnostic examination of cognitive heterogeneity in children and adolescents with neurodevelopmental disorders. *Child Neuropsychol* 2025; 31: 293–311.
16. Loo SK, Lenartowicz A, Makeig S. Research Review: Use of EEG biomarkers in child psychiatry research – current state and future directions. *J Child Psychol Psychiatry* 2016; 57: 4–17.
17. Neuhaus E, Lowry SJ, Santhosh M, Kresse A, Edwards LA, Keller J *et al.* Resting state EEG in youth with ASD: age, sex, and relation to phenotype. *J Neurodev Disord* 2021; 13: 33.
18. Wang J, Barstein J, Ethridge LE, Mosconi MW, Takarae Y, Sweeney JA. Resting state EEG abnormalities in autism spectrum disorders. *J Neurodev Disord* 2013; 5: 24.
19. Cohen MX. *Analyzing neural time series data: theory and practice*. MIT press, 2014.
20. Donoghue T, Haller M, Peterson EJ, Varma P, Sebastian P, Gao R *et al.* Parameterizing neural power spectra into periodic and aperiodic components. *Nat Neurosci* 2020; 23: 1655–1665.
21. Proteau-Lemieux M, Knoth IS, Davoudi S, Martin C-O, Bélanger A-M, Fontaine V *et al.* Specific EEG resting state biomarkers in FXS and ASD. *J Neurodev Disord* 2024; 16: 53.

22. Bosl W, Tierney A, Tager-Flusberg H, Nelson C. EEG complexity as a biomarker for autism spectrum disorder risk. *BMC Med* 2011; 9: 18.
23. França LGS, Miranda JGV, Leite M, Sharma NK, Walker MC, Lemieux L *et al.* Fractal and Multifractal Properties of Electrographic Recordings of Human Brain Activity: Toward Its Use as a Signal Feature for Machine Learning in Clinical Applications. *Front Physiol* 2018; Volume 9–2018. doi:10.3389/fphys.2018.01767.
24. Kesić S, Spasić SZ. Application of Higuchi's fractal dimension from basic to clinical neurophysiology: a review. *Comput Methods Programs Biomed* 2016; 133: 55–70.
25. Proteau-Lemieux M, Knoth IS, Davoudi S, Buckser R, Martin C-O, Bélanger A-M *et al.* Behavioral Phenotype Associations With Resting State EEG Signal Complexity and Power Spectral Density in Fragile X Syndrome. *Autism Res* 2026; 19: e70194.
26. Arutiunian V, Santhosh M, Neuhaus E, Borland H, Tompkins C, Bernier RA *et al.* The relationship between gamma-band neural oscillations and language skills in youth with Autism Spectrum Disorder and their first-degree relatives. *Mol Autism* 2024; 15: 19.
27. Bogéa Ribeiro L, da Silva Filho M. Systematic review on EEG analysis to diagnose and treat autism by evaluating functional connectivity and spectral power. *Neuropsychiatr Dis Treat* 2023;: 415–424.
28. Dubois AEE, Audet-Duchesne E, Knoth IS, Martin CO, Jizi K, Tamer P *et al.* Genetic modulation of brain dynamics in neurodevelopmental disorders: the impact of copy number variations on resting-state EEG. *Transl Psychiatry* 2025; 15: 139.
29. Karalunas S, Ostlund B, Alperin B, Figuracion M, Gustafsson H, Deming E *et al.* Electroencephalogram aperiodic power spectral slope can be reliably measured and predicts ADHD risk in early development. *Dev Psychobiol* 2022; 64 3. doi:10.1002/dev.22228.
30. Markovska-Simoska S, Pop-Jordanova N. Quantitative EEG in Children and Adults With Attention Deficit Hyperactivity Disorder. *Clin EEG Neurosci* 2017; 48: 20–32.
31. Ostlund B, Alperin B, Drew T, Karalunas S. Behavioral and cognitive correlates of the aperiodic (1/f-like) exponent of the EEG power spectrum in adolescents with and without ADHD. *Dev Cogn Neurosci* 2021; 48. doi:10.1016/j.dcn.2021.100931.
32. Robertson M, Furlong S, Voytek B, Donoghue T, Boettiger C, Sheridan M. EEG Power Spectral Slope differs by ADHD status and stimulant medication exposure in early childhood. *J Neurophysiol* 2019. doi:10.1152/jn.00388.2019.
33. Clarke AR, Barry RJ, McCarthy R, Selikowitz M. EEG-defined subtypes of children with attention-deficit/hyperactivity disorder. *Clin Neurophysiol* 2001; 112: 2098–105.
34. Horder J, Petrinovic MM, Mendez MA, Bruns A, Takumi T, Spooren W *et al.* Glutamate and GABA in autism spectrum disorder-a translational magnetic resonance spectroscopy study in man and rodent models. *Transl Psychiatry* 2018; 8: 106.
35. Simon DM, Wallace MT. Dysfunction of sensory oscillations in Autism Spectrum Disorder. *Neurosci Biobehav Rev* 2016; 68: 848–861.
36. Duffy FH, Als H. Autism, spectrum or clusters? An EEG coherence study. *BMC Neurol* 2019; 19: 27.

37. Adamou M, Fullen T, Jones SL. EEG for diagnosis of adult ADHD: a systematic review with narrative analysis. *Front Psychiatry* 2020; 11: 871.
38. Goodspeed K, Armstrong D, Dolce A, Evans P, Said R, Tsai P *et al.* Electroencephalographic (EEG) biomarkers in genetic neurodevelopmental disorders. *J Child Neurol* 2023; 38: 466–477.
39. Shephard E, Tye C, Ashwood KL, Azadi B, Asherson P, Bolton PF *et al.* Resting-State Neurophysiological Activity Patterns in Young People with ASD, ADHD, and ASD + ADHD. *J Autism Dev Disord* 2018; 48: 110–122.
40. Tombor L, Kakuszi B, Papp S, Réthelyi J, Bitter I, Czobor P. Decreased resting gamma activity in adult attention deficit/hyperactivity disorder. *World J Biol Psychiatry* 2019.
41. Orekhova EV, Stroganova TA, Prokofyev AO, Nygren G, Gillberg C, Elam M. Sensory gating in young children with autism: Relation to age, IQ, and EEG gamma oscillations. *Neurosci Lett* 2008; 434: 218–223.
42. Pierce S, Kadlaskar G, Edmondson DA, McNally Keehn R, Dydak U, Keehn B. Associations between sensory processing and electrophysiological and neurochemical measures in children with ASD: an EEG-MRS study. *J Neurodev Disord* 2021; 13: 5.
43. Bosl WJ, Tager-Flusberg H, Nelson CA. EEG Analytics for Early Detection of Autism Spectrum Disorder: A data-driven approach. *Sci Rep* 2018; 8: 6828.
44. Tenev A, Markovska-Simoska S, Müller A, Mishkovski I. Entropy, complexity, and spectral features of EEG signals in autism and typical development: a quantitative approach. *Front Psychiatry* 2025; 16: 1505297.
45. Mohammadi MR, Khaleghi A, Nasrabadi AM, Rafieivand S, Begol M, Zarafshan H. EEG classification of ADHD and normal children using non-linear features and neural network. *Biomed Eng Lett* 2016; 6: 66–73.
46. Duda M, Ma R, Haber N, Wall D. Use of machine learning for behavioral distinction of autism and ADHD. *Transl Psychiatry* 2016; 6: e732–e732.
47. Wolff N, Kohls G, Mack JT, Vahid A, Elster EM, Stroth S *et al.* A data driven machine learning approach to differentiate between autism spectrum disorder and attention-deficit/hyperactivity disorder based on the best-practice diagnostic instruments for autism. *Sci Rep* 2022; 12: 18744.
48. Rogala J, Żygierewicz J, Malinowska U, Cygan H, Stawicka E, Kobus A *et al.* Enhancing autism spectrum disorder classification in children through the integration of traditional statistics and classical machine learning techniques in EEG analysis. *Sci Rep* 2023; 13: 21748.
49. Jamal W, Das S, Oprescu I-A, Maharatna K, Apicella F, Sicca F. Classification of autism spectrum disorder using supervised learning of brain connectivity measures extracted from synchrostates. *J Neural Eng* 2014; 11: 046019.
50. Pham T-H, Vicnesh J, Wei JKE, Oh SL, Arunkumar N, Abdulhay EW *et al.* Autism spectrum disorder diagnostic system using HOS bispectrum with EEG signals. *Int J Environ Res Public Health* 2020; 17: 971.

51. Li L, Guo X, Yang Z, Zhao Y, Liu X, Yang J *et al.* ADHD detection from EEG signals using GCN based on multi-domain features. *Front Neurosci* 2025; 19: 1561994.
52. Lord C, Rutter M, DiLavore P, Risi S, Gotham K, Bishop S. Autism diagnostic observation schedule–2nd edition (ADOS-2). *Los Angel CA West Psychol Corp* 2012; 284: 474–478.
53. Wechsler D. Wechsler adult intelligence scale. *Arch Clin Neuropsychol* 1955.
54. Wechsler D. *WISC-V: Wechsler intelligence scale for children*. NCS Pearson, Incorporated, 2014.
55. Wechsler D. Wechsler preschool and primary scale of intelligence–revised. *J Sch Psychol* 1989.
56. Farmer C. Leiter International performance scale-revised (Leiter-R). In: *Encyclopedia of autism spectrum disorders*. Springer, 2021, pp 2701–2705.
57. Bruni TP. Test Review: Social Responsiveness Scale–Second Edition (SRS-2). *J Psychoeduc Assess* 2014; 32: 365–369.
58. Achenbach TM, Rescorla L. Child behavior checklist. *Burlington* 2000.
59. Gabard-Durnam LJ, Mendez Leal AS, Wilkinson CL, Levin AR. The Harvard Automated Processing Pipeline for Electroencephalography (HAPPE): standardized processing software for developmental and high-artifact data. *Front Neurosci* 2018; 12: 97.
60. Davoudi S, Arango GL, Deguire F, Knoth IS, Thebault-Dagher F, Reh R *et al.* Electroencephalography estimates brain age in infants with high precision: Leveraging advanced machine learning in healthcare. *NeuroImage* 2025; 312: 121200.
61. Vesanto J, Alhoniemi E. Clustering of the self-organizing map. *IEEE Trans Neural Netw* 2000; 11: 586–600.
62. Team RC. RA language and environment for statistical computing, R Foundation for Statistical. *Computing* 2020.
63. Hubert L, Arabie P. Comparing partitions. *J Classif* 1985; 2: 193–218.
64. Kohonen T. *Self-organizing maps*. Springer Science & Business Media, 2012.
65. Martinez S, Stoyanov K, Carcache L. Unraveling the spectrum: overlap, distinctions, and nuances of ADHD and ASD in children. *Front Psychiatry* 2024; 15: 1387179.
66. Tamon H, Fujino J, Itahashi T, Frahm L, Parlatini V, Aoki YY *et al.* Shared and specific neural correlates of attention deficit hyperactivity disorder and autism spectrum disorder: a meta-analysis of 243 task-based functional MRI studies. *Am J Psychiatry* 2024; 181: 541–552.
67. Constantino JN, Davis SA, Todd RD, Schindler MK, Gross MM, Brophy SL *et al.* Validation of a brief quantitative measure of autistic traits: comparison of the social responsiveness scale with the autism diagnostic interview-revised. *J Autism Dev Disord* 2003; 33: 427–433.
68. Campbell IG, Feinberg I. Longitudinal trajectories of non-rapid eye movement delta and theta EEG as indicators of adolescent brain maturation. *Proc Natl Acad Sci* 2009; 106: 5177–5180.
69. Giraud A-L, Poeppel D. Cortical oscillations and speech processing: emerging computational principles and operations. *Nat Neurosci* 2012; 15: 511–517.

70. Fries P. Neuronal gamma-band synchronization as a fundamental process in cortical computation. *Annu Rev Neurosci* 2009; 32: 209–224.
71. Neo WS, Foti D, Keehn B, Kelleher B. Resting-state EEG power differences in autism spectrum disorder: a systematic review and meta-analysis. *Transl Psychiatry* 2023; 13: 389.
72. Sohal VS, Rubenstein JLR. Excitation-inhibition balance as a framework for investigating mechanisms in neuropsychiatric disorders. *Mol Psychiatry* 2019; 24: 1248–1257.
73. Rubenstein J, Merzenich MM. Model of autism: increased ratio of excitation/inhibition in key neural systems. *Genes Brain Behav* 2003; 2: 255–267.
74. Nelson SB, Valakh V. Excitatory/inhibitory balance and circuit homeostasis in autism spectrum disorders. *Neuron* 2015; 87: 684–698.
75. Antoine MW, Langberg T, Schnepel P, Feldman DE. Increased excitation-inhibition ratio stabilizes synapse and circuit excitability in four autism mouse models. *neuron* 2019; 101: 648–661. e4.
76. Latrèche K, Godel M, Flò A, Journal F, Borghesani V, Schaer M. Early Trajectories of Resting-State EEG power in autistic children: a longitudinal study across language profiles. *Transl Psychiatry* 2026. doi:10.1038/s41398-026-04132-0.
77. Devarajan K, Jyostna E, Jayasri K, Balasampath V. EEG-based epilepsy detection and prediction. *Int J Eng Technol* 2014; 6: 212.
78. Córdova F. On the meaning of Hurst entropy applied to EEG data series. *Procedia Comput Sci* 2022; 199: 1385–1392.
79. Linkenkaer-Hansen K, Smit DJ, Barkil A, van Beijsterveldt TE, Brussaard AB, Boomsma DI *et al*. Genetic contributions to long-range temporal correlations in ongoing oscillations. *J Neurosci* 2007; 27: 13882–13889.
80. Higuchi T. Approach to an irregular time series on the basis of the fractal theory. *Phys Nonlinear Phenom* 1988; 31: 277–283.
81. Eke A, Herman P, Kocsis L, Kozak L. Fractal characterization of complexity in temporal physiological signals. *Physiol Meas* 2002; 23: R1–R38.
82. Croce P, Zappasodi F. Complexity and Persistence of Electrical Brain Activity Estimated by Higuchi Fractal Dimension. *Fractal Fract* 2026; 10: 88.
83. Wolfson SS, Kirk I, Waldie K, King C. EEG Complexity Analysis of Brain States, Tasks and ASD Risk. In: Di Ieva A (ed). *The Fractal Geometry of the Brain*. Springer International Publishing: Cham, 2024, pp 733–759.

Tables

Tables 1 to 4 are available in the Supplementary Files section.

Figures

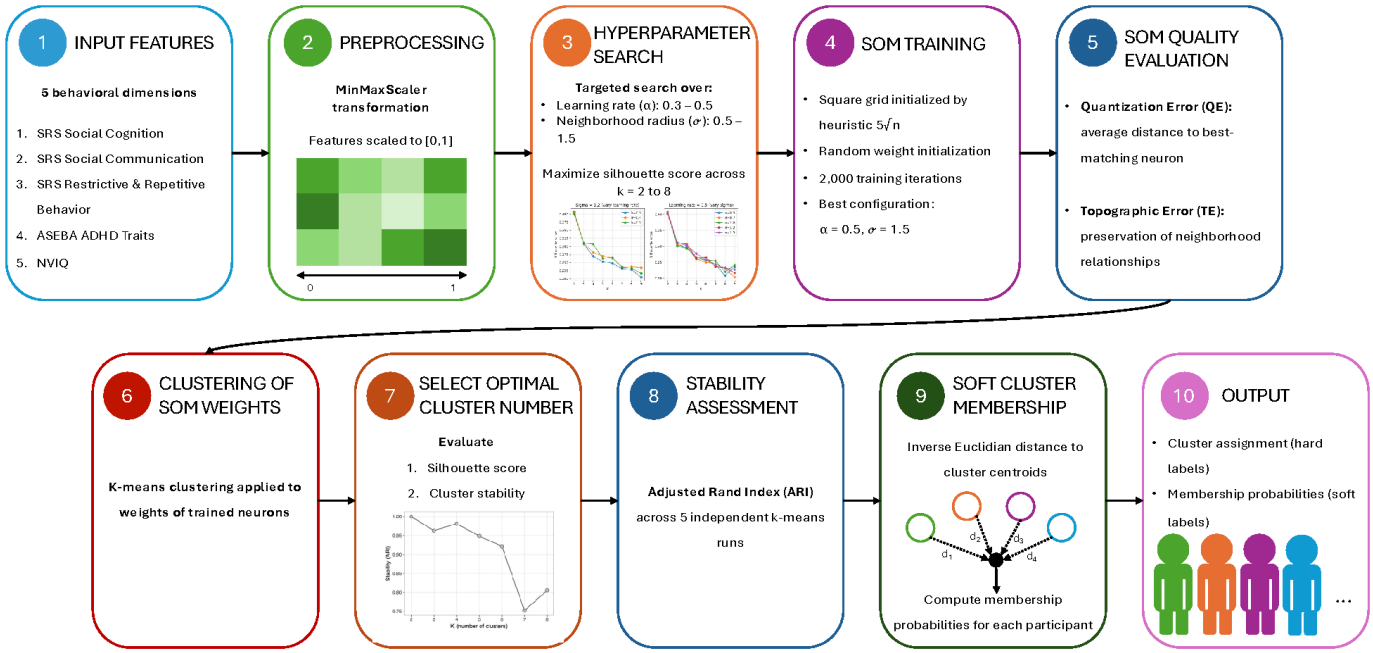


Figure 1

Legend not included with this version.

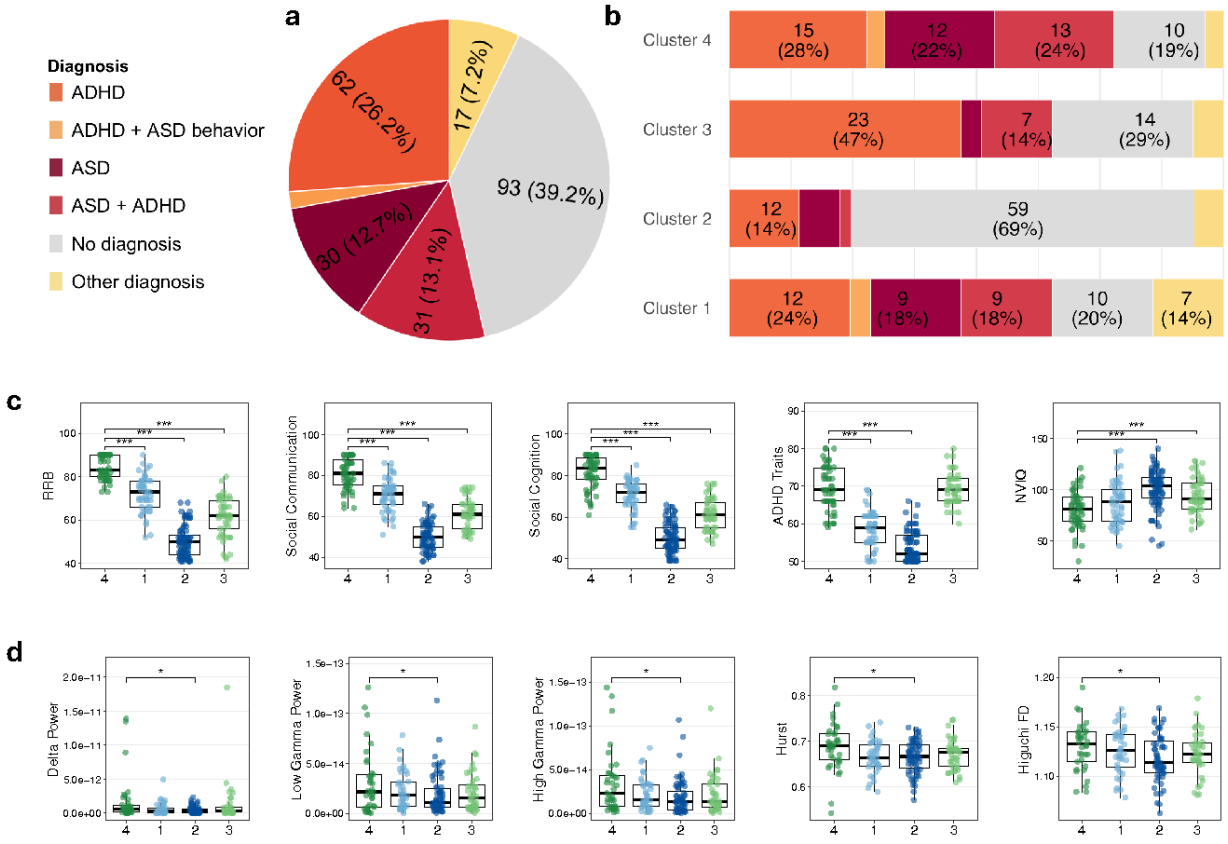


Figure 2

Legend not included with this version.

Supplementary Files

This is a list of supplementary files associated with this preprint. Click to download.

- Table1.pdf
- Table2.pdf
- Table3.pdf
- Table4.pdf
- SupplementalMaterial.docx